Robotica (2017) volume 35, pp. 166–188. © Cambridge University Press 2015
doi:10.1017/S0263574715000077

Determination of the initial conditions by solving boundary value problem method for period-one walking of a passive biped walking robots

Masoumeh Safartoobi, Morteza Dardel*, Mohammad Hassan Ghasemi and Hamidreza Mohammadi Daniali

Department of Mechanical Engineering, Babol Noshirvani University of Technology, P.O. Box 484, Postal Code: 47148-71167, Shariati Street, Babol, Mazandaran, Iran

(Accepted 16 January 2015. First published online: March 13, 2015)

SUMMARY

With regard to the small basin of attraction of the passive limit cycles, it is important to start from a proper initial condition for stable walking. The present study investigates the passive dynamic behaviors of two-dimensional bipedal walkers of a compass gait model with different foot shapes. In order to find proper initial conditions for stable and unstable period-one gait limit cycles, a method based on solving the nonlinear equations of motion is presented as a boundary value problem (BVP). An initial guess is required to solve the related BVP that is obtained by solving an initial value problem (IVP). For parametric analysis purposes, a continuation method is applied. Simulation results reveal two, period-one gait cycles and the effects of parameters variation for all models.

KEYWORDS: Passive dynamic; Bipedal walker; Initial conditions; Period-one gait limit cycle.

1. Introduction

Stable walking is one of the most important activities in our daily life. However, walking is a very complicated dynamic phenomenon and has not been very well understood. Bipeds represent a class of legged robots that attempt to imitate the human style of locomotion. Designing biped robots from a human-like walking perspective has particular importance in the field of robotics and the prosthetics industry. Biped locomotion is one sophisticated form of legged locomotion. Perhaps the simplest model which has been used to study some basic features of human locomotion is the simple two-link inverted pendulum. This passive legged mechanism which can easily perform a steady gait cycle on a shallow slope, was first initiated by McGeer in the 1990s.[1,2] Unlike traditional humanoid robots, that use actuated joints to control every motion,[3–5] this passive dynamic walker utilizes gravity as its source of energy. The energy lost due to friction and collisions can be compensated by the potential energy. McGeer's results suggest that the mechanical parameters of the human body such as leg lengths and their mass distributions affect the gate quality.[6] Inspired by the work of McGeer, researchers studied many different simple to complex biped robots in order to achieve passive walking. Goswami *et al.*[7] introduced the compass gait biped robot with point feet. Garcia *et al.*[8] introduced a design of passive walkers with two massless links and a hip mass that could walk on arbitrarily shallow slopes. Both of these popular models are studied for local stability and bifurcation routes to chaos based on the change in the slope angle. Wisse *et al.*[9] and Kumar *et al.*[10] studied a stable passive walker with upper body and toed feet. Moreover, Safa *et al.*[11] studied the motion of Garcia's simplest model on stairs instead of ramps. The search for cyclic motions in the passive bipedal walking is a root-finding problem using a map, which was first done by Hurmuzlu.[12] This map function is generally called a Poincare map, which is used to analyze walking motions.[1,8,13] Fixed points of the Poincare map are computed using Newton–Raphson method from a good estimate of the initial condition achieved

* Corresponding author. E-mail: dardel@nit.ac.ir

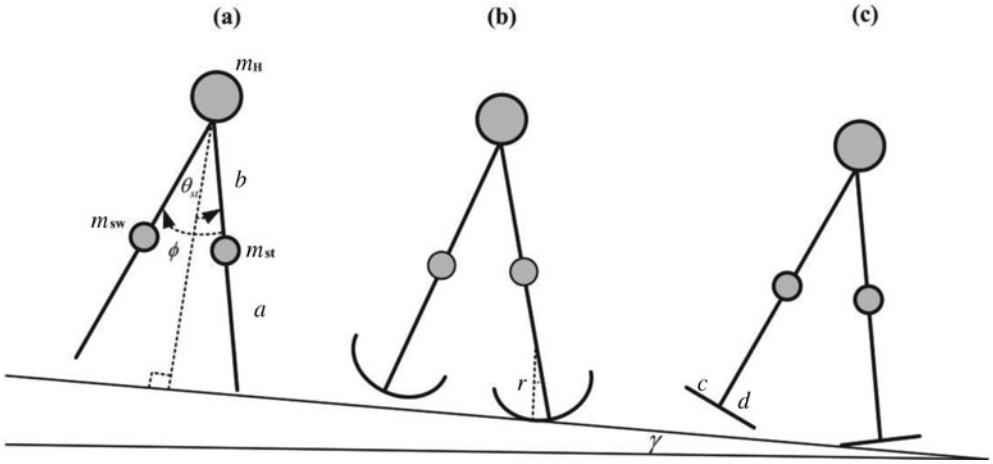

Fig. 1. Different models of the compass gait biped robot (a) point feet, (b) curved feet, and (c) flat feet.

from the nonlinear equations of the walking motion.[14,15] Indeed, these points are periodic solutions that yield periodic gaits. It is noted that, the eigenvalues of the Jacobian matrix around these fixed points of the Poincare map define the stability of the gait cycle. A stable periodic gait exists, if a passive walker starts walking from the neighborhood of these stable fixed points. All the possible initial conditions for a stable walking motion are in the basin of attraction of the stable gait, which contains the fixed points. The basin of attraction of the walker is a small region and decreases as the slope angle increases.[16,17]

In order to prevent falling forward or backward, it is important to start with proper initial conditions. Garcia *et al*.[8] found the proper initial conditions of the simplest walking model using the linearized equations of motion. Other researchers proposed a simple search algorithm to find a set of the initial conditions that result in stable limit cycles for various parameter values.[18] Recently, Jeon *et al*.[19] applied falling boundary and energy balance line to estimate the proper initial conditions. These set of initial conditions are within the basin of attraction of the stable gait cycle. It is noteworthy that the basin of attraction is small, then the passive bipeds have many walking limitations. In addition, these walkers cannot walk on level ground and their motions on shallow slopes are with low speeds.[20] However, the effort to generate pretty human-like gaits with low energy consumption has increased the importance of the passive dynamic walker. From this point of view, the significant role of foot shape in the walking process was studied through simulations and experiments.[18,21,22] The study of passive dynamic behavior is possible by solving their nonlinear differential equations. However, analytical solutions of these equations are difficult for biped models with different foot shapes.

Finding the proper initial conditions for a stable periodic gait in the passive bipedal walking is very important and requires a new numerical solution. Therefore, this research proposes a new approach to get the initial conditions for stable and even unstable period-one gait limit cycles of all compass gait models with different foot shapes such as curved and flat feet. Using continuation method, the effects of physical parameters variation are investigated, as well.

2. Theoretical Analysis

2.1. The passive biped dynamic walkers

2.1.1. Models. Goswami *et al*.[13] considered the simple passive compass gait biped robot. Biped robots with different foot shapes are shown in Fig. 1. Two kinds of feet including curved and flat feet are added to the basic model studied by Goswami. The physical parameters of these models are denoted in Fig. 1, in which r is the radius of the curved foot. For the flat feet model with fixed ankle, c is the distance between the ankle and the end of heel, and d is the distance between the ankle and the end of toe. When r in Fig. 1b, or c and d in Fig. 1c vanishes, these models become the simple passive compass gait model with point feet. Also the subscripts st and sw indicates the stance leg and the swing leg, respectively.

https://doi.org/10.1017/S0263574715000077 Published online by Cambridge University Press

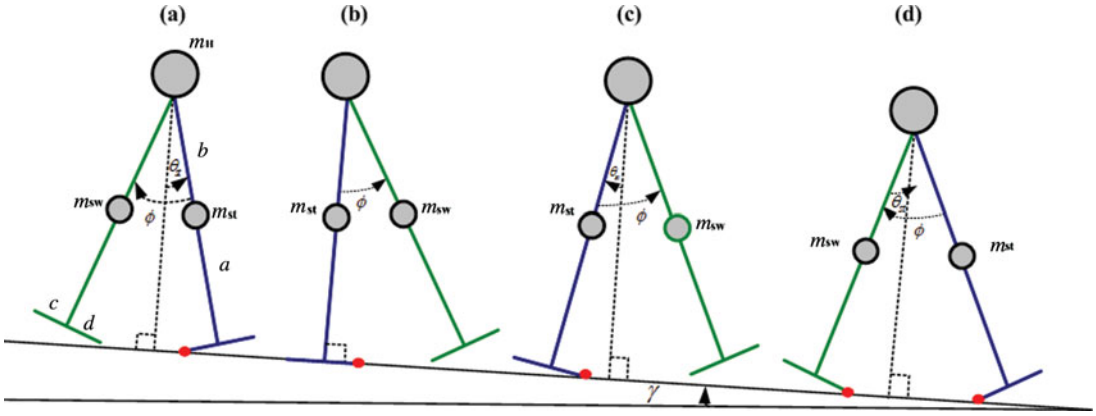

Fig. 2. The flat feet model (a) 1st swing phase 1, (b) 1st transition, (c) 2nd swing phase, and (d) 2nd transition.

These models have two symmetric legs, which are rigidly connected by a frictionless hinge joint at the hip, allowing them to swing freely. There are three point-masses, one for the hip and the other two for the legs. At the start of each step, the gait consists of double support. The basic model walks passively down the rigid ramp of slope γ in two-dimensional space with suitable initial conditions. During swing phase, the entire stance leg acts as an inverted pendulum pivoting around its foot. The swing leg is represented as a free pendulum pivoting around the hip until it reaches the slope surface at the end of each step. The scuffing problem of the swing leg is neglected at the mid-stance. It is assumed that, there is no slip and no bounce at the pivot point. Then, the roles of the two legs will be changed. The equations of motion of the swing phase together with the transition rule are needed to describe the dynamics behavior of the models. The transition role is obtained by using conservation of angular momentum and geometric collision conditions.

2.1.2. Dynamic equations of motion for the swing phase. The equations of motion between collisions can be determined by using the well-known Lagrange–Euler equations. The models have two degrees of freedom, i.e. θ_{st} and ϕ. θ_{st} is the angle of the stance leg with normal to the slope surface, while ϕ is the angle between the stance and the swing legs. To simplify the governing equations, following assumptions and dimensionless parameters are introduced.

$$m_{st} = m_{sw} = m, \beta = \frac{m}{m_H}, \quad \tau = \sqrt{\frac{g}{l}}t, \bar{a} = \frac{a}{l}, \quad \bar{b} = \frac{b}{l}, \quad \bar{r} = \frac{r}{l}, \quad \bar{c} = \frac{c}{l}, \quad \bar{d} = \frac{d}{l}, \tag{1}$$

where β is the mass ratio and τ is the dimensionless time. Therefore, the dimensionless equations describing the dynamics of pendulum motion are given by:

$$\boldsymbol{M}_n(\boldsymbol{\theta})\ddot{\boldsymbol{\theta}} + \boldsymbol{C}_n\left(\boldsymbol{\theta}, \dot{\boldsymbol{\theta}}\right)\dot{\boldsymbol{\theta}} + \boldsymbol{g}_n(\boldsymbol{\theta}) = 0, \tag{2}$$

where $\theta = [\,\theta_{st}\ \phi\,]^T$, $M_n(\theta)$ is the inertia matrix, $C_n(\theta, \dot{\theta})$ is the centrifugal and Coriolis terms, and $g_n(\theta)$ is the gravitational vector. The dimensionless matrices for the three biped models of Fig. 1 are given in Appendix A.1.

The swing phase for the flat feet model can be divided into two phases. As illustrated in Fig. 2a, at the first swing phase, the heel of the stance leg acts as a hinge. The first swing phase appears similarly in the models with the point feet and the curved feet. When the toe of the stance leg touches a ramp, the second swing phase will be started as shown in Fig. 2b. These swing phases have nearly similar dynamics equations and the only difference is in the change in switching pivot point from the heel to the toe. Thus, the dimensionless matrices of the second swing phase can be used after replacing $\bar{c}$ with $-\bar{d}$.

Moreover, the equations of motion of the flat and the curved feet models are the same as the basic model when their feet shape parameters vanishes.

https://doi.org/10.1017/S0263574715000077 Published online by Cambridge University Press

2.1.3. Transition rules at collision. The collision occurs when the swing leg touches the ramp surface and the former stance leg leaves the slope in the same instant. Therefore, the swing leg becomes the new stance leg and vice versa. This instantaneous impact is assumed to be plastic without slipping. The effect of collisions, which appears in the initial values and includes leg angles and angular velocities, is called transition rules. Thus, the transition rules of angular velocities can be derived by applying the conservation law of the angular momentum about the hip and the impact points, i.e.

$$Q_n^- \begin{bmatrix} \dot{\theta}_{\mathrm{st}} \\ \dot{\phi} \end{bmatrix}^- = Q_n^+ \begin{bmatrix} \dot{\theta}_{\mathrm{st}} \\ \dot{\phi} \end{bmatrix}^+, \tag{3}$$

where Q_n^- and Q_n^+ are both square matrices given in appendix A. 1. The superscripts "–" and "+" denote immediately before and after the collision, respectively. Moreover, the normalized matrices Q_n^- and Q_n^+ can be found in Appendix A. 2. At each step, for the point and curved feet models there is only one collision and one heel-strike, whereas the flat feet model has two collisions. At the end of the first swing phase, the contact point changes from the heel to the toe of the stance leg. After rotating on the toe, the heel-strike occurs at the end of the second swing phase. For the simple compass gait model, the heel-strike can be modeled by the following geometric collision condition.

$$\phi - 2\theta_{\mathrm{st}} = 0. \tag{4}$$

By employing the geometric relations, the transition rules of the angular displacement are given as J, in the following equation.

$$\begin{bmatrix} \theta_{\mathrm{st}} \\ \phi \end{bmatrix}^+ = \begin{bmatrix} -1 & 0 \\ -2 & 0 \end{bmatrix}_J \begin{bmatrix} \theta_{\mathrm{st}} \\ \phi \end{bmatrix}^-. \tag{5}$$

For the curved feet model, the geometric collision condition and the transition rules of angular displacement are similar to the basic model. For the flat feet model, the geometric collision relation of the toe-strike is defined when the angle of the stance leg vanishes. If this is the case, the angular relationship before and after the collision is given in the square matrix J as follows:

$$\begin{bmatrix} \theta_{\mathrm{st}} \\ \phi \end{bmatrix}^+ = \begin{bmatrix} 1 & 0 \\ 0 & 1 \end{bmatrix} \begin{bmatrix} \theta_{\mathrm{st}} \\ \phi \end{bmatrix}^-. \tag{6}$$

Each step starts and ends with the heel-strike. For the flat feet model, if the ankle parameters of c and d are chosen equal, the geometric collision condition of the heel-strike is the same as the heel-strike of the point and curved feet models. Consequently, for all biped models the whole transition rules are identified with the following matrix:

$$q^+ = \begin{bmatrix} J & 0 \\ 0 & \left(Q_n^+\right)^{-1} Q_n^- \end{bmatrix} q^-, \tag{7}$$

with $q = [\theta_{\mathrm{st}}, \phi, \dot{\theta}_{\mathrm{st}}, \dot{\phi}]^T$. The above expression reveals that the state vector after collision, which is taken as a new initial condition for the next step is determined by a map function. This function is defined as a solution of the governing equations when it meets the collision condition.

2.2. Finding the proper initial conditions and period-one gait cycles

The motion of the biped models is switching between two dynamics parts. The first part is a time-continuous gait including the motion of swing phase. The second part is the discrete collision events. The differential equations cannot be solved continuously in according to the collision events. In fact, they should be solved by using the transition rules that describe the relations between the state vector before and after the collision. To get a stable gait cycle, it is needed to solve the equations of the swing phase and the transition rules with appropriate initial conditions. Since it is difficult

https://doi.org/10.1017/S0263574715000077 Published online by Cambridge University Press

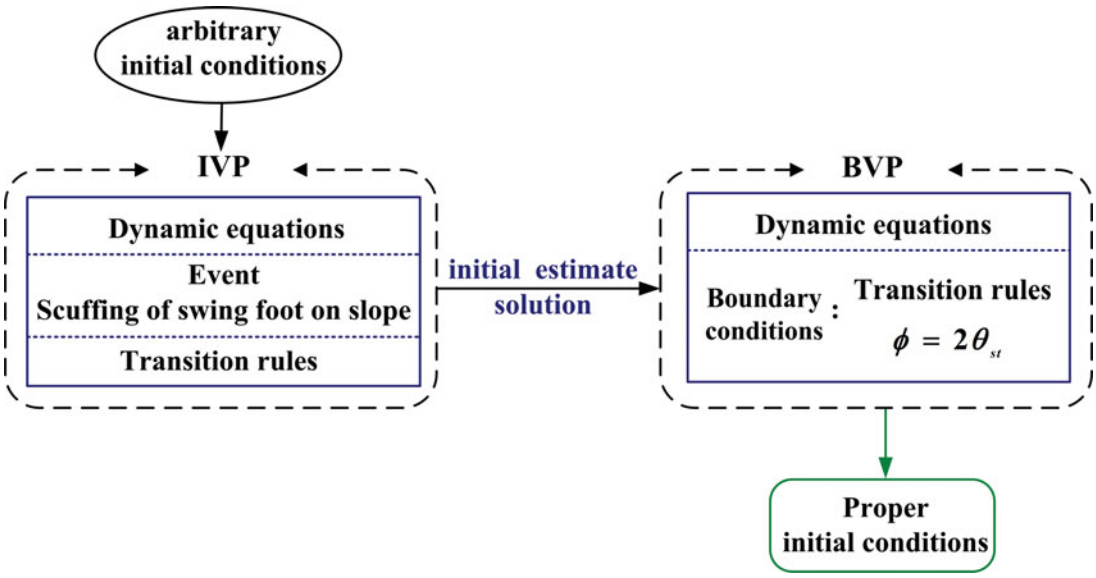

Fig. 3. The outline of the proposed method for determination of appropriate initial conditions.

to analytically solve the governing equations, usually in dynamical systems, numerically iterative searching algorithm is used for finding periodic motions. Using perturbation method, Garcia *et al.* determined the leg angles and velocities at the fixed points.[8] But it is difficult to apply this method for biped models with the curved or flat feet shapes. Using the gait cycle as a function of the slope surface, Garcia *et al.* found period-one limit cycles.[8] Their methods based on making the Poincare map can be time consuming, especially in bipeds with complex gait patterns. Finding two periodic solutions (long and short) is another problem in applying these solution procedures. To overcome difficulties in obtaining appropriate initial conditions for a stable and unstable gait cycles, the basic idea of the proposed algorithm is explained in the followings.

In general, the nonlinear equations of the biped robots can be solved conceptually in the form of a BVP in which the angle and angular velocities define the boundary conditions. The following form can define the state-space representation of equation of motion for the biped robots with different foot shapes.

$$\dot{q} = \frac{d}{dt}\begin{pmatrix}\theta\\ \dot{\theta}\end{pmatrix} = \begin{pmatrix}\dot{\theta}\\ -M_n^{-1}(\theta)\left[C_n\left(\theta,\dot{\theta}\right)\dot{\theta} + g_n(\theta)\right]\end{pmatrix} \tag{8}$$

$$q(t=0) = q^+, \quad q(t=T) = q^-.$$

Using the dimensionless time $\tau = t/T$, where T is the step period, Eq. (8) can be rewritten as follows:

$$q' = \frac{d}{d\tau}\begin{pmatrix}\theta\\ \theta'\end{pmatrix} = T\begin{pmatrix}\theta'\\ -M_n^{-1}(\theta)\left[C_n\left(\theta,\theta'\right)\theta' + g_n(\theta)\right]\end{pmatrix}$$

$$q(\tau=0) = \begin{bmatrix}\theta_{\mathrm{st}} & \phi & \theta'_{\mathrm{st}} & \phi'\end{bmatrix}^+, \quad q(\tau=1) = \begin{bmatrix}\theta_{st} & \phi & \theta'_{\mathrm{st}} & \phi'\end{bmatrix}^- . \tag{9}$$

In order to determine the boundary conditions in one-step, it is necessary to include transition rule at the collision point of Eq. (7). However, it is difficult to solve the nonlinear BVP if there is no closed-form solution for it. In this work, the proposed method to determine initial conditions of stable and unstable period-one limit cycles is based on the well capabilities of MATLAB or other numerical softwares in solving different differential equations such as ordinary differential equation (ODE) or IVP, BVP, differential delay equation (DDE) and etc.[23] There are different algorithms such as Runge–Kutta's method for solving ODEs in MATLAB that can solve stiff and non-stiff problems with a desired accuracy. Also, MATLAB offers various integrator options such as EVENT option to

https://doi.org/10.1017/S0263574715000077 Published online by Cambridge University Press

Table I. Physical parameters of the investigated cases.

Simplest walking model	Foot shape parameter		Slope angle
Point feet	$\bar{a} = 0$	$\bar{r} = 0, \bar{c} + \bar{d} = 0$	0.009 rad
Curved feet		$\bar{r} = 0.05$	
Flat feet		$\bar{c} = \bar{d} = 0.0001$	0.001 rad

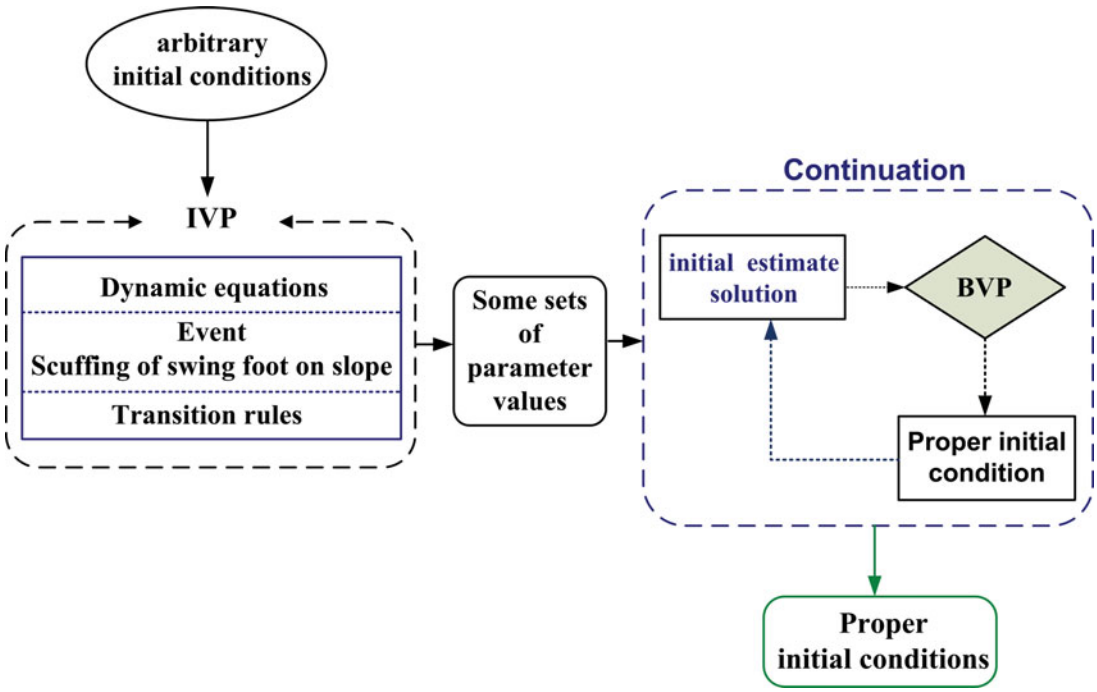

Fig. 4. Schematic structure of the continuation method.

improve the ODE solver performance.[23] This option acts as a function that can be used for different objectives such constructing a Poincare map, or if statement. Moreover, MATLAB uses collocation technique for numerically solving BVP, but solving BVP needs a good initial estimate for the desired solution. With regard to the collisions or jump conditions in the biped models, solving the BVP is not easy. To overcome these difficulties, the proposed approach combines the MATLAB capabilities in solving ODE and BVP to obtain the appropriate initial conditions or the gait cycles. The general procedure to obtain the period-one gait cycle for different biped models is explained as following.

As mentioned earlier, solving the equations of motion at swing phases and the equations of impact form a BVP. In other hand, the overall model of the biped walking along with the initial conditions forms an IVP. The solution of this IVP results in a periodic gait if the walker goes down a slope with an appropriate initial conditions. Since a BVP might have multiple solutions, MATLAB BVP solvers such as bvp4c, bvp5c or bvp6c require an initial guess.[23] Moreover, it is necessary that the initial guess be as close as to the true solution of BVP. For this purpose, by using ODE numerical solution methods such as ode45 of MATLAB, the solution of an IVP can be a good initial guess to BVP. The IVP also needs an initial guess (value) to be proceeded by time. It is much better to choose this arbitrary initial guess from small values. For calculating a cyclic solution, it is necessary to stop the solution at a specific conditions and applying the transition rule given by Eq. (7) at the end of this cycle. This termination condition is called an "event" in MATLAB ODE solver. For all models, the "event" can be defined as the time when the swing leg scuffs with the slope surface. This situation can be occurred in any time, even at the mid-stance of the swing phase. The models with point and

https://doi.org/10.1017/S0263574715000077 Published online by Cambridge University Press

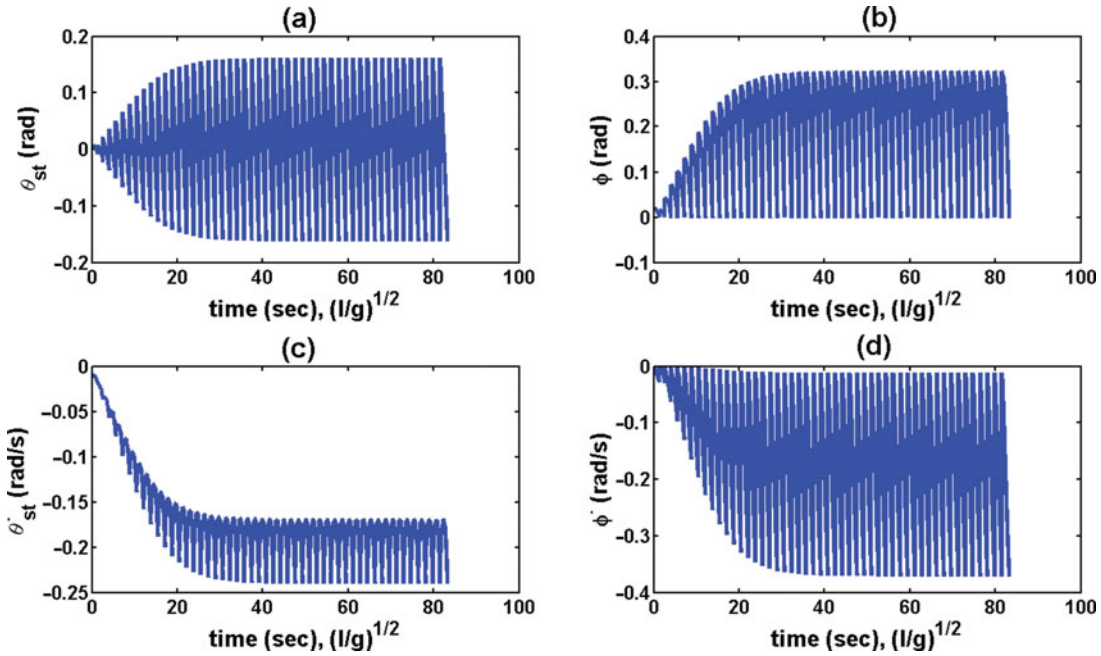

Fig. 5. Suitable initial estimate of BVP for point feet model at long period from solving IVP with swing leg scuffing event condition ($\gamma = 0.009$ rad).

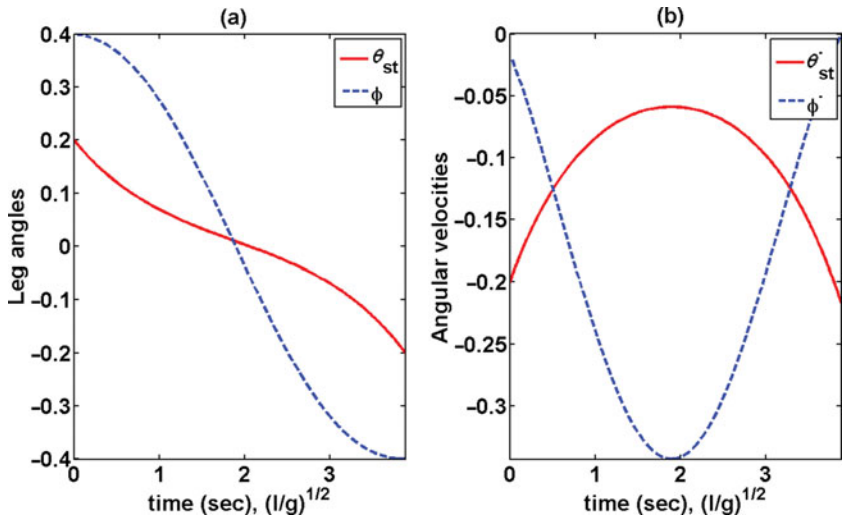

Fig. 6. Proper initial condition for the simplest model with point feet at long period ($\gamma = 0.009$ rad).

curved feet have the same impact event that is given by

$$l\left(\cos\theta_{st} - \cos\left(\phi - \theta_{st}\right)\right) = 0. \tag{10}$$

As mentioned earlier, there are two impact events for the flat feet model as defined by the following expressions:

$$\begin{aligned} &\left(\bar{c} + \bar{d}\right)\sin\theta_{st} = 0 \\ &\bar{c}\sin\theta_{st} + \cos\theta_{st} - \bar{d}\sin(\phi - \theta_{st}) - \cos(\phi - \theta_{st}) = 0. \end{aligned} \tag{11}$$

https://doi.org/10.1017/S0263574715000077 Published online by Cambridge University Press

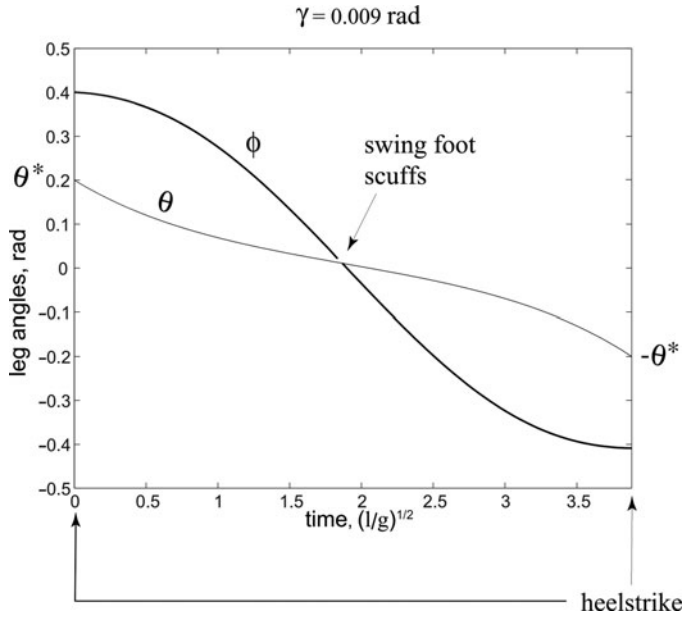

Fig. 7. Leg angles vs. time over one-step at a long-period gait cycle obtained by Garcia *et al*.[8]

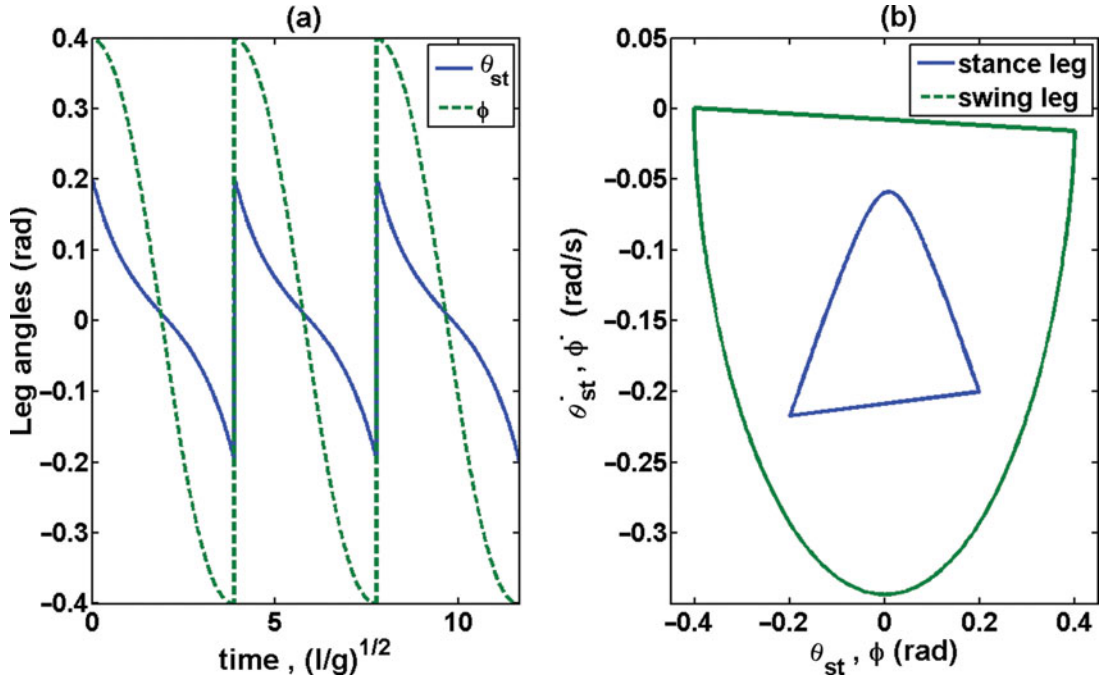

Fig. 8. (a) Leg angles vs. time over three steps at a long period gait cycle, (b) limit cycle in phase plane of the point feet model ($\gamma = 0.009$ rad).

Now, the transition rule is applied to the solution at the point of the swing foot scuff with the slope surface. Next, with this obtained initial condition, the solution of the ODE problem is preceded with time until at the steady state a periodic solution is obtained. This periodic solution is not the true gait cycle or the solution of BVP, since at the end of each step the true solution must justify the condition of $\phi = 2\theta_{st}$. Since the periodic solution of the ODE problem, at least can satisfy the equations of motion or the transition rules, it is a very good initial solution for the BVP. Then, by applying this initial solution to the BVP solvers such as bvp4c of MATLAB, an accurate solution

https://doi.org/10.1017/S0263574715000077 Published online by Cambridge University Press

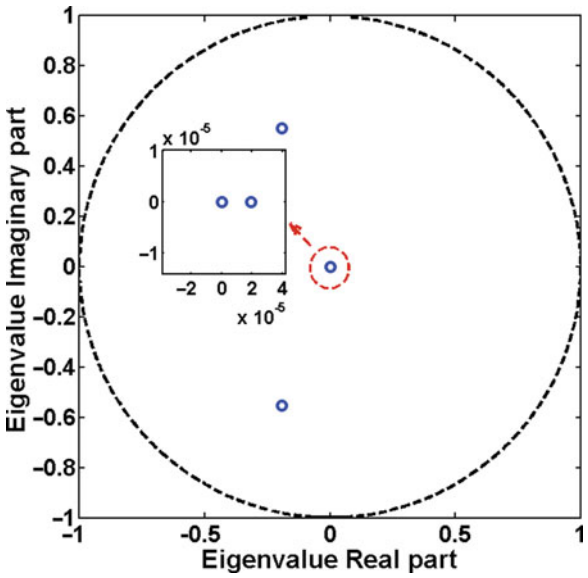

Fig. 9. Loci of eigenvalues for the point feet model at long period-one gait cycle ($\gamma = 0.009$ rad).

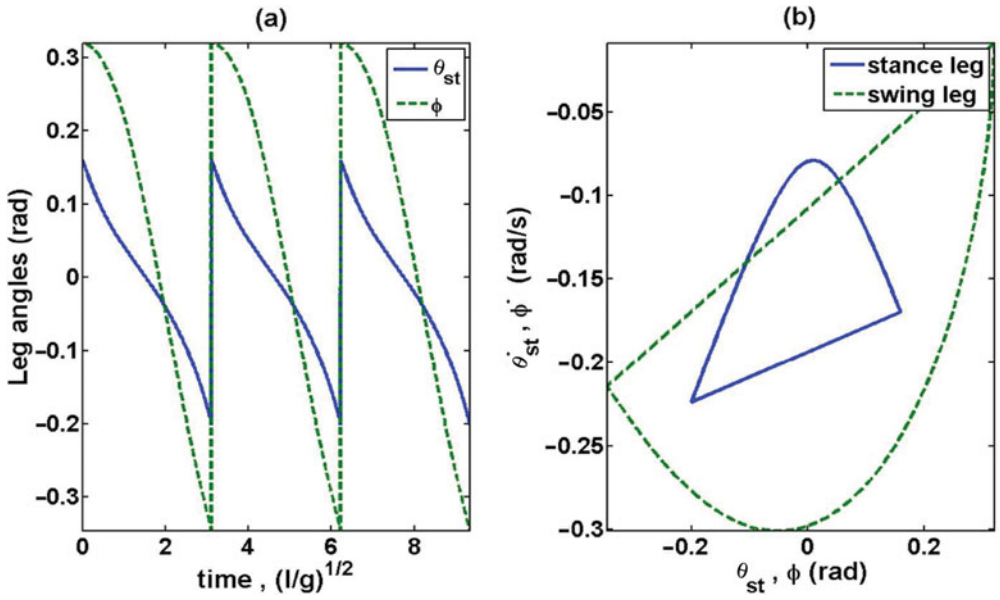

Fig. 10. (a) Short period-one gait cycle, (b) limit cycle in phase plane of the point feet model ($\gamma = 0.009$ rad).

of the problem can be obtained. This output provides the appropriate initial conditions for the stable and the unstable period-one gait cycles. It is noted that for all biped models, the BVP must uses the true collision conditions at the end of each step. The outline of the proposed algorithm for finding the initial conditions of the limit cycles of biped robot is illustrated in Fig. 3.

Upon finding the initial conditions, the walker's periodic gait can be simulated by integrating the equations of the swing phase and applying the transition rules at true collision condition. This simulation forms an IVP by defining the event as the time when $\phi = 2\theta_{st}$ and the initial conditions as an initial value. As opposed to the previous studies which require defining Poincare map in their solving processes, here the fixed points or periodic gaits can be found directly without defining such map. Numerical calculations found two period-one solutions to this IVP as short period and long period gait cycles based on different initial conditions.

https://doi.org/10.1017/S0263574715000077 Published online by Cambridge University Press

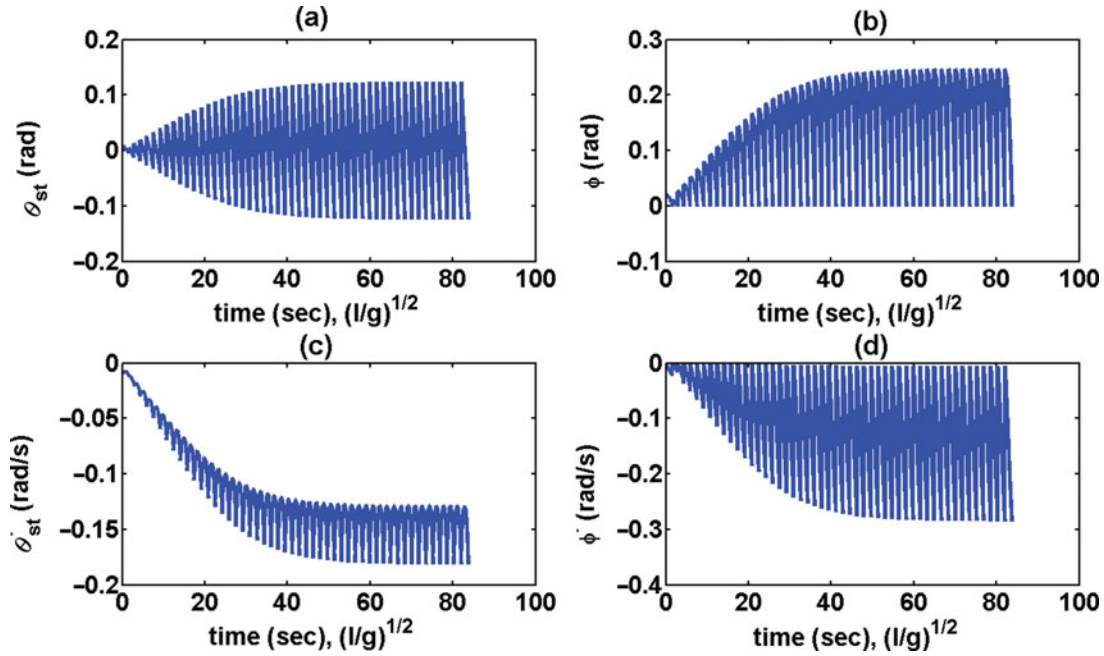

Fig. 11. Suitable initial estimate of BVP for the point feet model at long period from solving IVP with swing leg scuffing event condition ($\gamma = 0.004$ rad).

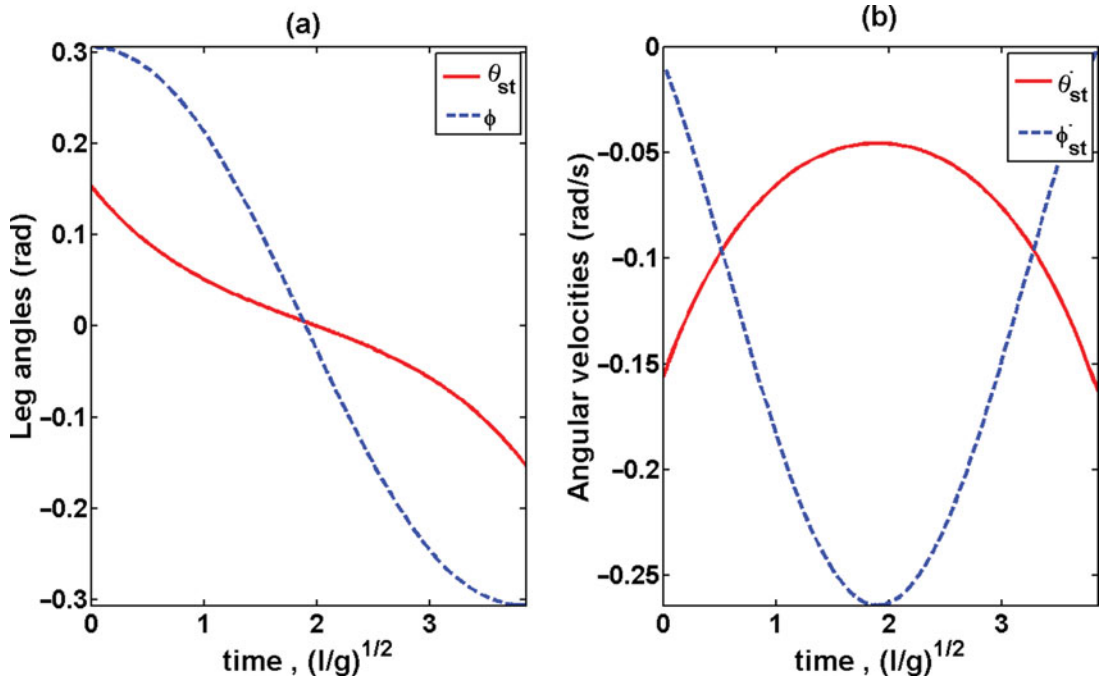

Fig. 12. Proper initial condition for the point feet model at long period ($\gamma = 0.004$ rad).

2.3. Stability analysis

The local stability of a limit cycle walking can be analyzed around the fixed points on the Poincare map by evaluating the eigenvalues of the Jacobian matrix.[8] If the eigenvalues of the Jacobian matrix are inside the unit circle in the complex plane, the limit cycle is stable. Garcia *et al*. found the Jacobian by both numerical and analytic procedure.[8] This approach calculates the Jacobian matrix by simulating one step for a small perturbation on each of the states of the fixed points.

https://doi.org/10.1017/S0263574715000077 Published online by Cambridge University Press

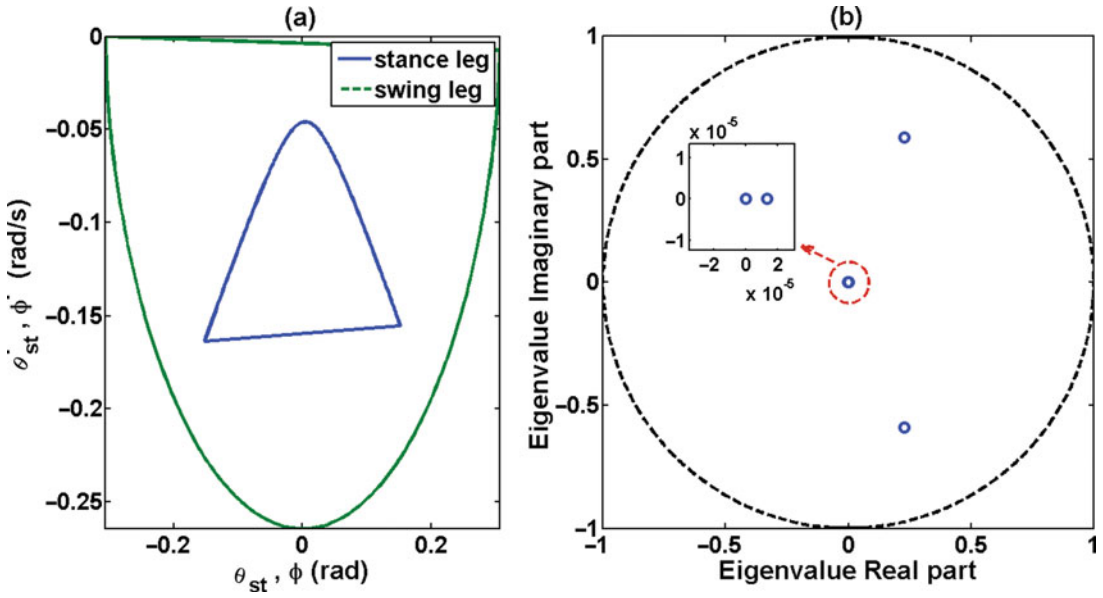

Fig. 13. (a) Long period limit cycle, (b) loci of eigenvalues for the point feet model ($\gamma = 0.004$ rad).

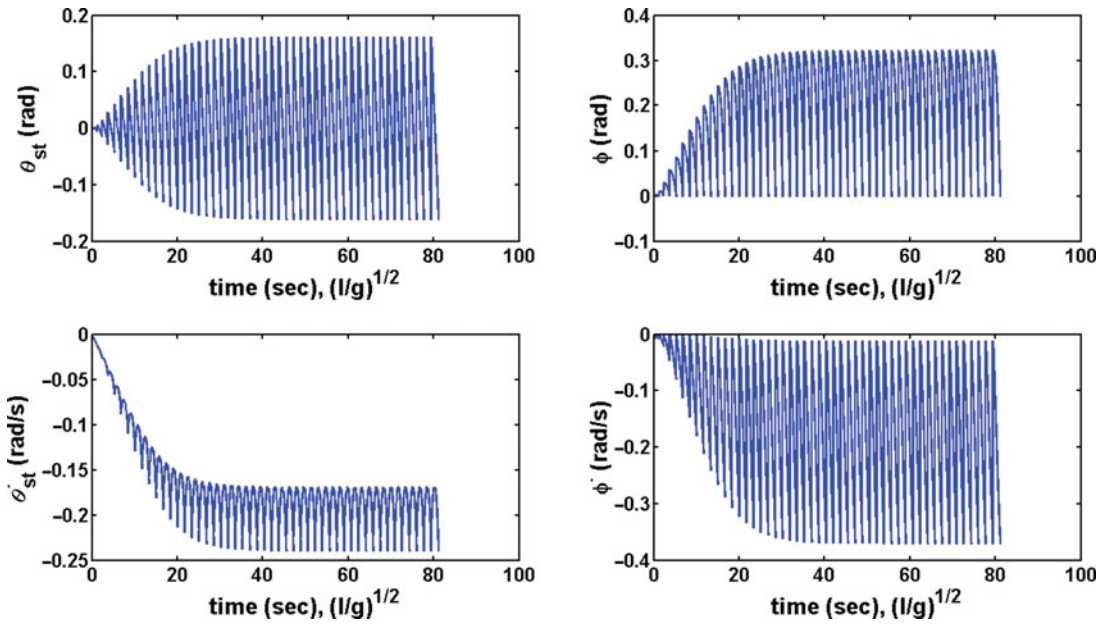

Fig. 14. Suitable initial estimate of BVP for the curved feet model at long period from solving IVP with swing leg scuffing event condition ($\gamma = 0.009$ rad).

2.4. Parameter study

Upon applying the proposed algorithm and obtaining the initial conditions for the gait cycle of the passive walker, it is necessary to provide an initial guess for other sets of parameter values, as well. This can be done by investigating the effect of varying parameters on the limit cycle behavior of the biped models. Continuation method, which solves the problem as a sequence of relatively simpler problems, is used here to simply solving a BVP. To obtain the initial conditions for different parameters of the robot under study here, continuation method in according to Fig. 4 uses an available solution of the BVP for biped with given parameter value as the initial guess for the next value.

https://doi.org/10.1017/S0263574715000077 Published online by Cambridge University Press

Table II. Three cases for investigating parameters variation.

Simplest walking models	Parameter values		
Point feet	$\beta = 0$	$\bar{a} = 0$	$\gamma = [0.009 : 0.01 : 0.015]$
Curved feet		$\bar{a} = 0, \gamma = 0.009$	$r = [0 : 0.01 : 0.15]$

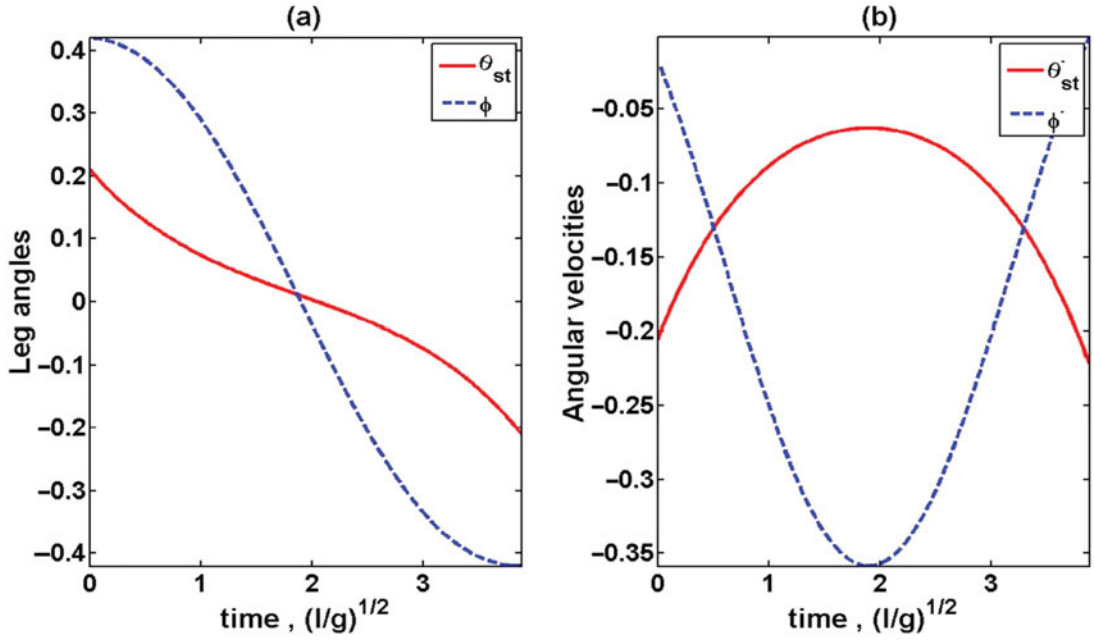

Fig. 15. Proper initial condition for the curved feet model at long period ($\gamma = 0.009$ rad).

3. Simulations

3.1. Finding the period-one gait cycles

In this subsection, the period-one gait cycles are determined by using the suggested algorithm to find the proper initial conditions for all the models. Obviously, when the distance between the foot and hip and the mass ratio are close to zero, the simple compass gait model becomes the simplest walking model conceived by Garcia *et al*.[8] By applying the presented method on the different cases of Table I, simulation results are discussed as following.

Figures 5 and 6 show how the suitable guess and the proper initial conditions are obtained for the simplest walking model with point feet, respectively. Firstly, in according to the proposed solution procedure, the problem is solved as an IVP with an arbitrary initial guess and the event condition of scuffing the swing leg. By applying the transition rule to the state at the instant of swing leg scuffs with surface, and using them as an initial guesses and continuing the solution of IVP with time, a periodic solution will be obtained, as shown in Fig. 5. As seen from Fig. 5a, the solution of the stance leg has similar form with its real gait (although its amplitude and period are different with the true solution), but the solution of the swing leg is different from what is expected for the true solution. Now, by selecting the end cycle of this periodic solution as an initial solution guess of BVP with true jump condition, accurate solution of the problem related to the initial conditions can be obtained, as shown in Fig. 6. Moreover, Fig. 6 is completely similar with Garcia's obtained result shown in Fig. 7. This is a long period gait. This result shows the good performance of the proposed algorithm.

The obtained result for a long period-one gait limit cycle with step period $T = 3.882$ is shown in Fig. 8. The initial conditions of the point feet model are found as $[\theta_{st}^*, \phi^*, \dot{\theta}_{st}^*, \dot{\phi}^*] = [0.2003, 0.40062, -0.19983, -0.01582]$. The corresponding eigenvalues of the Jacobian matrix for this gait cycle are $[-0.193 \pm 0.554i, 0, 0]$. As anticipated, all of these eigenvalues are inside the unit circle shown in Fig. 9. It means that the long period-one limit cycle of the point feet model is stable. Also the point feet model has a short period-one gait cycle with step period $T = 3.112$ as

https://doi.org/10.1017/S0263574715000077 Published online by Cambridge University Press

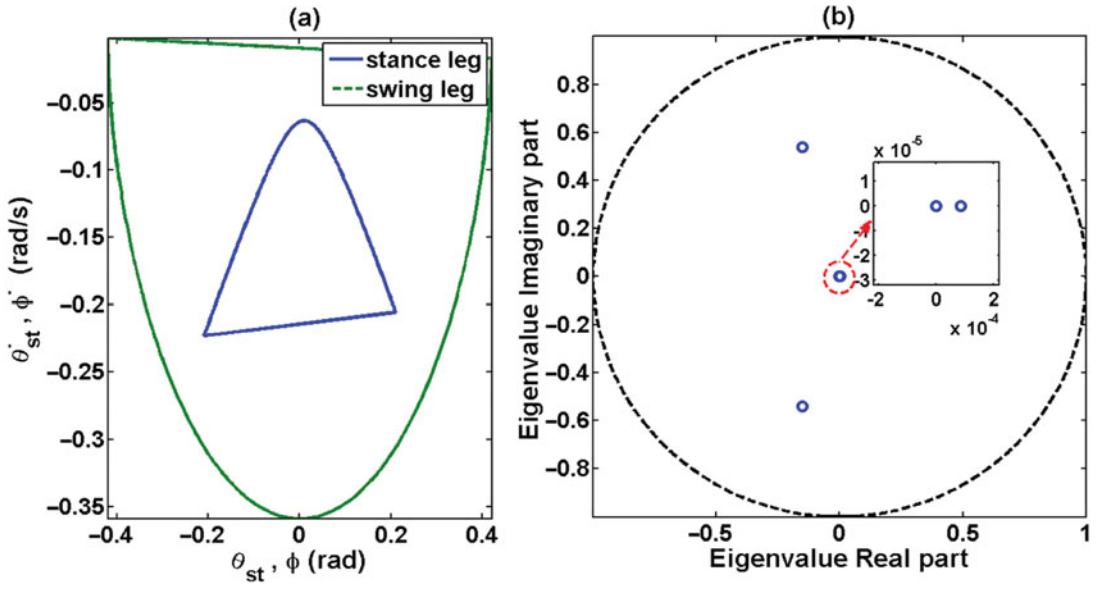

Fig. 16. (a) Long period-one limit cycle, (b) loci of eigenvalues for the curved feet model ($\gamma = 0.009$ rad).

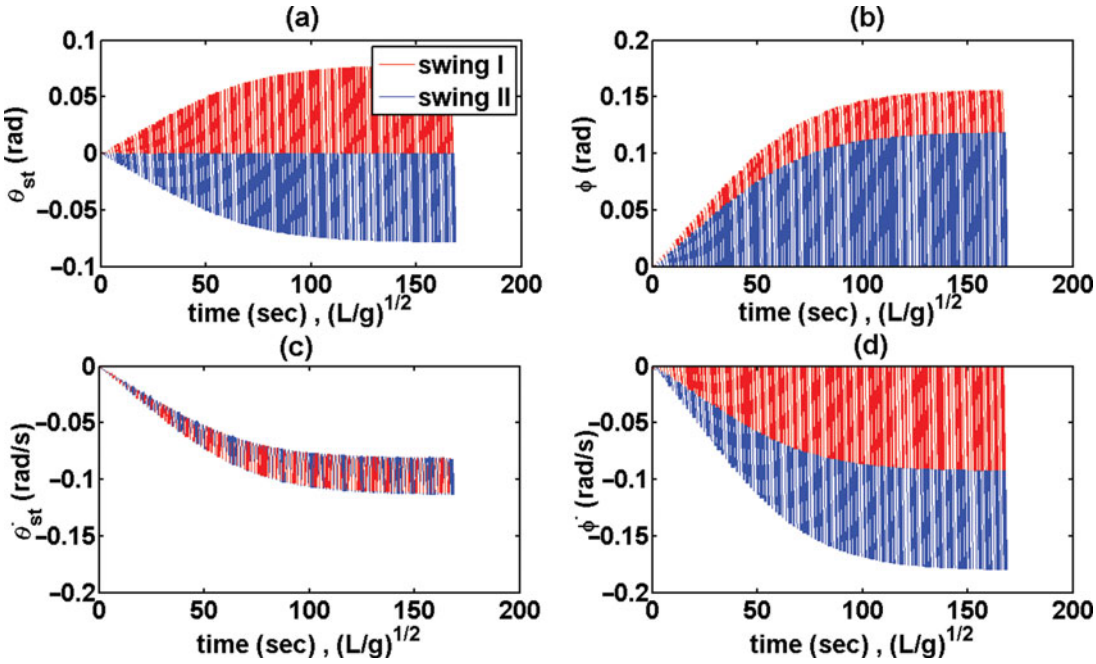

Fig. 17. Suitable initial estimate of BVP for the flat feet model at short period from solving IVP with swing leg scuffing event condition ($\gamma = 0.001$ rad).

shown in Fig. 10. The initial conditions of this gait cycle are $\left[\theta_{st}^*, \phi^*, \dot{\theta}_{st}^*, \dot{\phi}^*\right] = [0.165, 0.40062, -0.19983, -0.01582]$. For this gait cycle, one of the eigenvalues has magnitude greater than 1. This result implies that the short period-one limit cycle is unstable. It is noted that Garcia's simplest waking model exhibits two period-one gait cycles, one of them is stable for $0 < \gamma < 0.015$ rad.[8] Appendix B contains all necessary MATLAB M-files to obtain the stable and the unstable period-one gait cycles of the point feet biped model.

The above simulations of the point feet model also repeated for the slope angle of 0.004 rad, and the obtained results are shown in Figs. 11–13. In this case, the initial conditions were determined as $[\theta_{st}^*, \phi^*, \dot{\theta}_{st}^*, \dot{\phi}^*] = [0.1534, 0.3068, -0.1561, -0.0073]$. The eigenvalues of the Jacobian matrix

https://doi.org/10.1017/S0263574715000077 Published online by Cambridge University Press

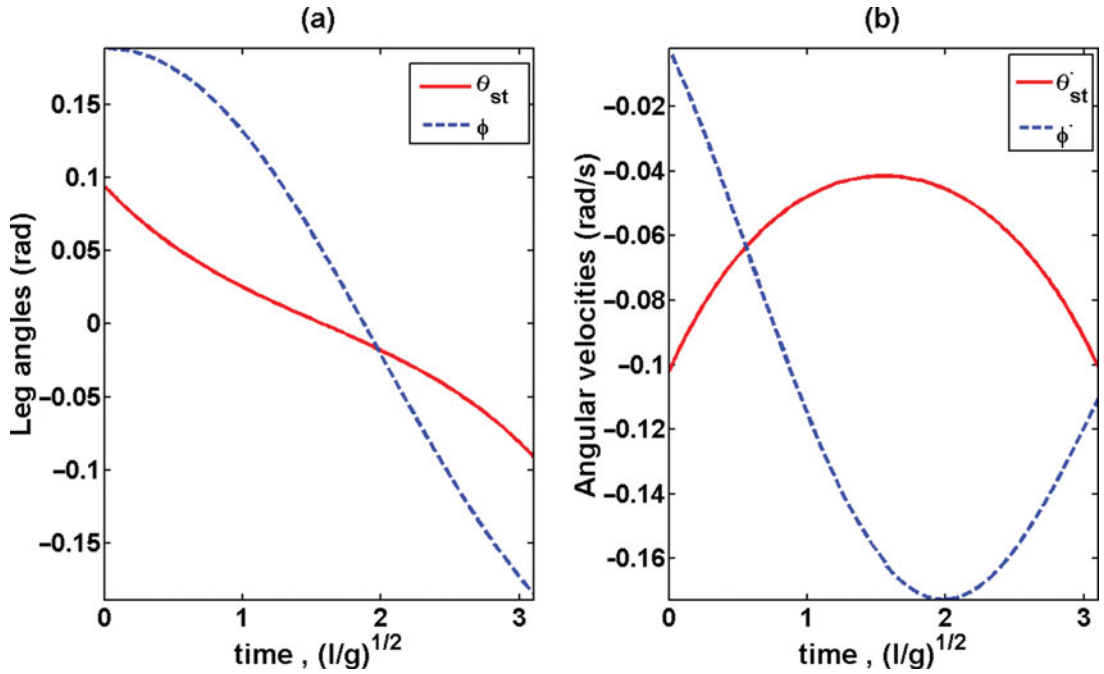

Fig. 18. Proper initial condition for the flat feet model at short period ($\gamma = 0.001$ rad).

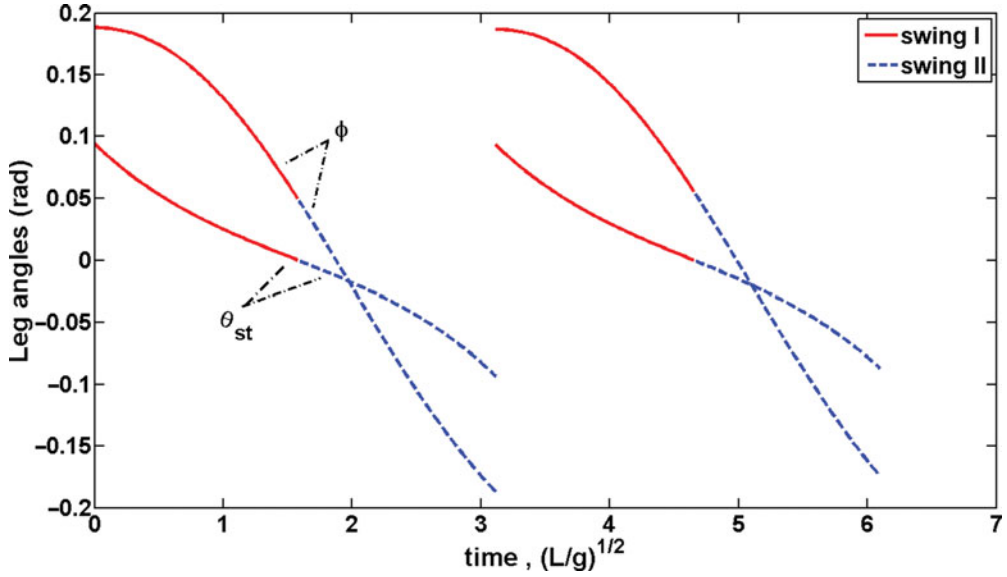

Fig. 19. Leg angles vs. time over two step at a short period-one gait cycle for the flat feet model ($\gamma = 0.001$ rad).

are $[-0.23 \pm 0.59\text{i}, 0, 0]$. The loci of eigenvalues in Fig. 13b, exhibits the stable long period-one limit cycle of the point feed biped robot.

The proposed algorithm is repeated for the curve feet model with the specification given in Table I. The initial estimated BVP solution and the long period-one gait cycle are shown in Figs. 14 and 15, respectively. Since the radius of the curved foot is very small, the gait cycle for this model is nearly the same as that for the point feet model. From Fig. 16, it is observed that the simplest walking model with curved feet has stable long period-one limit cycle.

There are two period-one gait cycles for the flat feet biped model of Table I. This section focuses on the short period-one gait cycle of the flat feet model. As mentioned in Section 2, one step motion of this model is divided into four phases consisting of two swing phases and two collisions. The

https://doi.org/10.1017/S0263574715000077 Published online by Cambridge University Press

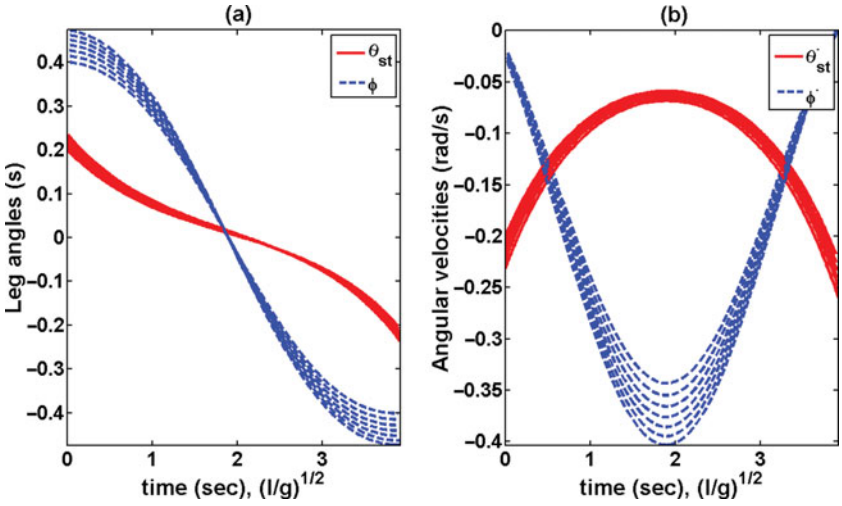

Fig. 20. Gait cycles of the point feet model for $\gamma = [0.009 : 0.01 : 0.015]$.

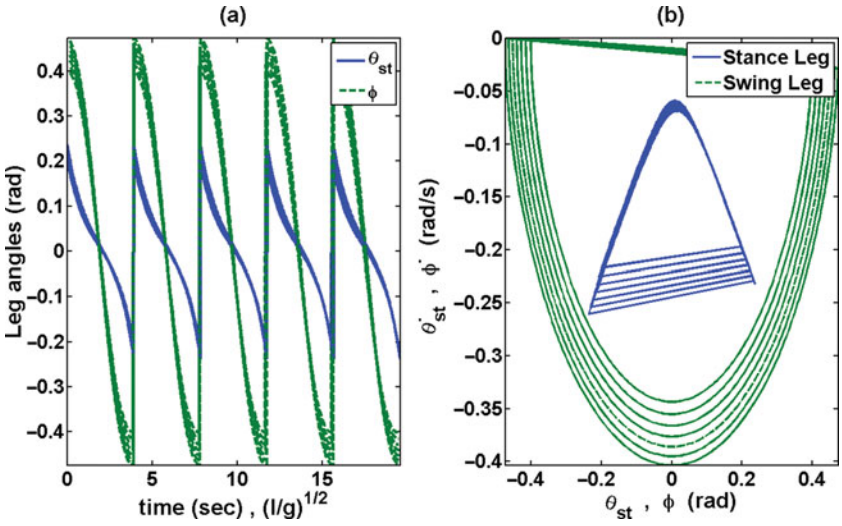

Fig. 21. (a) Long period-one gait cycles, and (b) limit cycles in phase plane, for the point feet biped model with slope angles of $\gamma = [0.009 : 0.01 : 0.015]$.

suitable initial estimated BVP solution is provided in Fig. 17. The proper initial conditions and the two steps of the flat feet model at short period are shown in Figs. 18 and 19.

Figures 9, 13 and 16 clearly reveals that the long period-one gait cycles of all models in Table I are stable, whereas the short ones are unstable.

3.2. Effect of varying different parameters

In this subsection, the effect of varying parameters, as given in Table II, on the limit cycle behavior of the point feet and the curved feet walking robots are studied.

3.2.1. Point feet model: slope angle γ. The continuation method uses the output of BVP for the slope 0.009 rad at the long period gait as the initial guess for the next slope. Then by continuously changing the slope angle, the long period-one gait limit cycles for other parameters are obtained. The gait cycles for all slope angles are shown in Figs. 20 and 21.

Figure 22 shows the changes of the initial conditions or the fixed points versus slope angles for the point feet biped model. With increase in the slope angle, the leg angles increase while their angular velocities decrease. Also the stability analysis is done for small perturbations around these points. For the range of the slope angles where the eigenvalues are smaller than unity, the point feet model has a stable walking. According to the simulation results of Fig. 23, the stable long period-one gait

https://doi.org/10.1017/S0263574715000077 Published online by Cambridge University Press

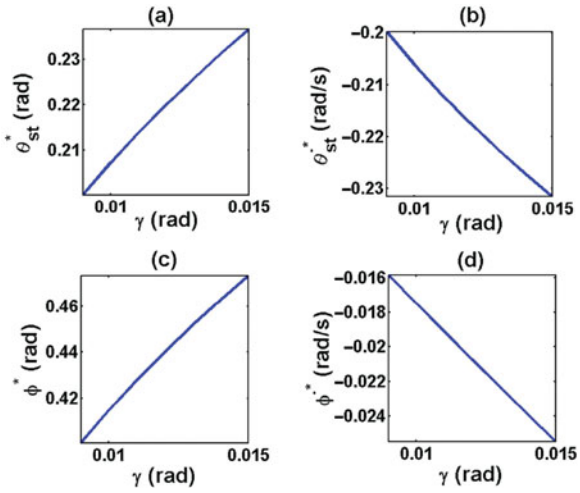

Fig. 22. Variation of the fixed points vs. slope γ for the point feet model.

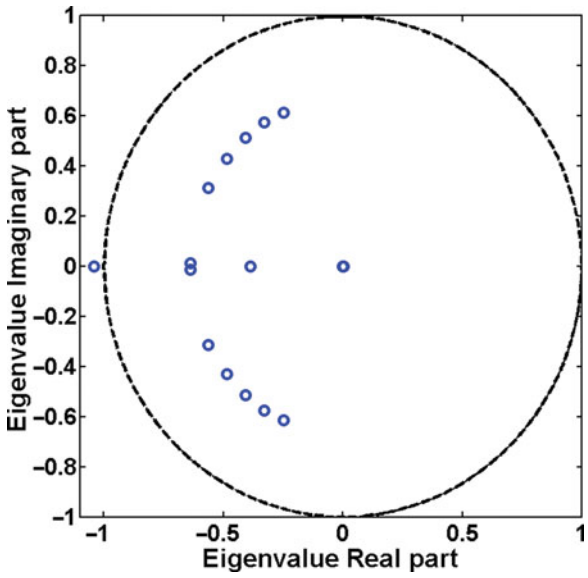

Fig. 23. Loci of eigenvalues for the point feet model for $\gamma = [0.009 : 0.01 : 0.015]$.

cycle exists for $0 < \gamma < 0.015$ rad. When $\gamma = 0.015$ rad, one of the eigenvalues is greater than unity; therefore the period one gait cycle looses stability.

3.2.2. The curved feet model: foot parameter $\bar{r}$. Using the model presented in Table I and applying the continuation algorithm, the effects of the varying foot parameter $\bar{r}$ for the curved shape biped robot are investigated, as well. The solutions of BVP and the one step gait cycle are shown in Fig. 24. Using these initial conditions, the long period-one gait cycles and limit cycles in phase plane are obtained and illustrated in Fig. 25.

Moreover, the variations of the calculated fixed points are shown in Fig. 26. These results imply that with increase in radius, the leg angles at the fixed points increase, but the angular velocities at these points decrease. Also the loci of the corresponding eigenvalues, as illustrated in Fig. 27, show that these limit cycles are stable.

4. Conclusion

In this work, compass gait biped robot with three different foot shapes has been studied. Initial conditions have been found for the stable and unstable period-one gait limit cycles by solving the

https://doi.org/10.1017/S0263574715000077 Published online by Cambridge University Press

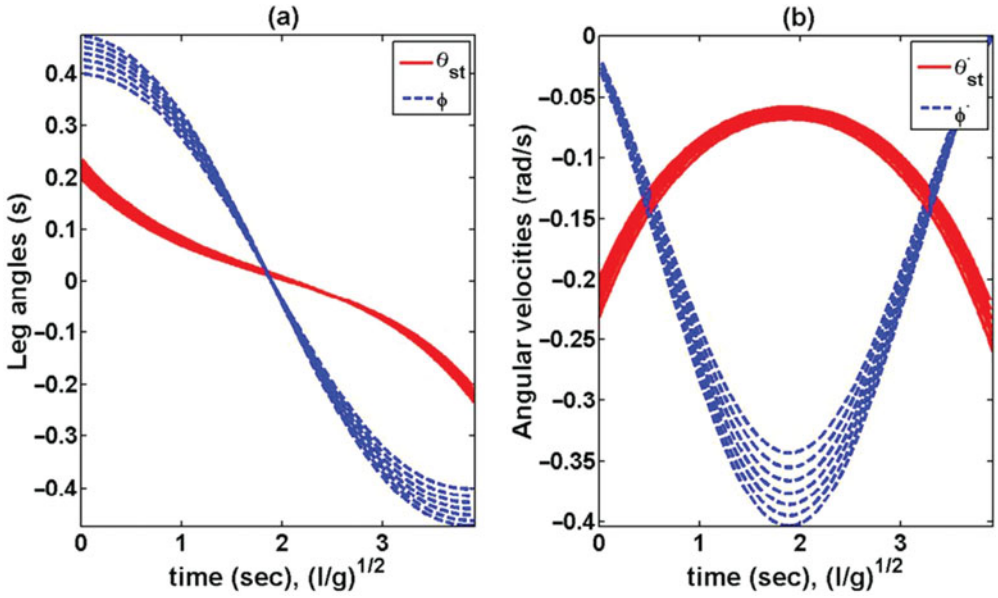

Fig. 24. Initial conditions of the curved feet model for $\bar{r} = [0 : 0.01 : 0.15]$.

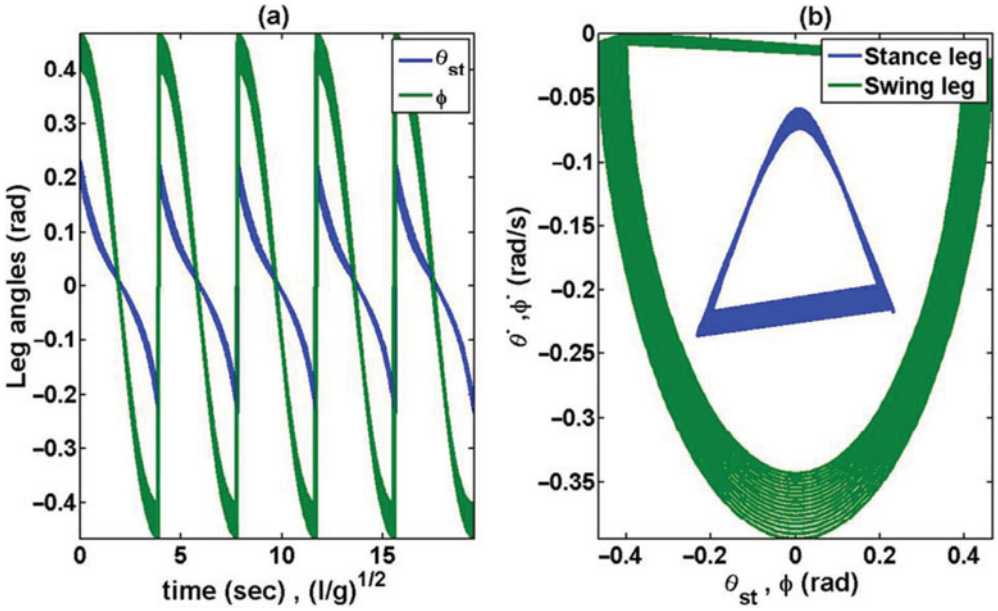

Fig. 25. (a) Long period-one gait cycles, (b) limit cycles in phase plane on the range of radius.

nonlinear equations of motion as a BVP. The appropriate initial guess for this BVP has been determined by the periodic output of solving the equations as an IVP with a small arbitrary initial guess. In the solving process, it has been required to locate points where the swing leg scuffs with slope surface, which can be defined as an event collision. After finding the initial conditions, the walker's periodic gait has been simulated by integrating the equations of the swing phase and applying a transition rule at $\phi = 2\theta_{st}$. The existence of the two period-one gait limit cycles has been confirmed through calculations of the proposed algorithm for three models. The fixed points have been computed in the small neighborhood of the proper initial conditions without using the Poincare map. Moreover, the continuation method has been presented to quantify the effects of variation of physical parameters on the stability of limit cycle. This method has been applied to get the proper initial conditions for some sets of slope angles and radii of the point and curved feet models, respectively.

https://doi.org/10.1017/S0263574715000077 Published online by Cambridge University Press

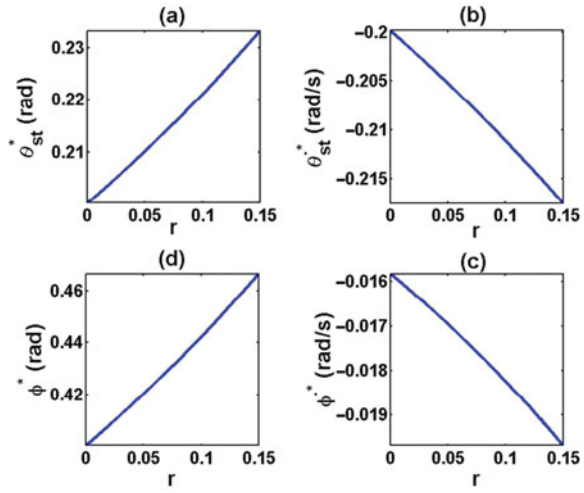

Fig. 26. Variation of fixed points vs. $\bar{r}$ for the curved feet model ($\gamma = 0.009$ rad).

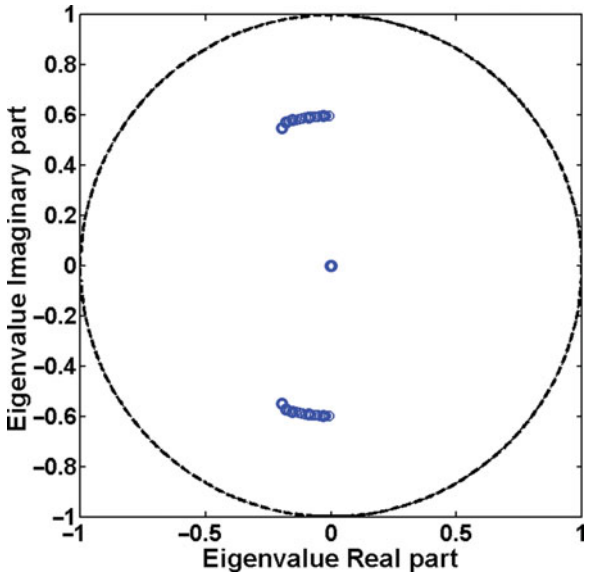

Fig. 27. Loci of eigenvalues for various $\bar{r}$ of the curved feet biped model.

References

1. T. McGeer, "Passive dynamic walking," *Int. J. Robot. Res.* **9**(2), 62–68 (1990).
2. T. McGeer, "Passive Walking with Knees," *Proceedings of the IEEE Conference on Robotics and Automation* (ICRA), Cincinnati, OH, USA; 13 May 1990 through 18 May 1990; Vol. 13 (1990), pp. 1640–1645.
3. K. Nariokaa and K. Hosodab, "Designing synergistic walking of a whole-body humanoid driven by pneumatic artificial muscles: An empirical study," *Adv. Robot.* **22**(10), 1107–1123 (2008).
4. B. Vanderborghta, R. Van Hamb, B. Verrelstc, M. Van Dammed and D. Lefebere, "Overview of the Lucy project: Dynamic stabilization of a biped powered by pneumatic artificial muscles," *Adv. Robot.* **22**(10), 1027–1051 (2008).
5. K. Hosoda, T. Takuma, A. Nakamoto and S. Hayashi, "Biped robot design powered by antagonistic pneumatic actuators for multi-modal locomotion," *Robot. Auton. Syst.* **56**, 46–53 (2008).
6. Q. Li and X.-S. Yang, "New walking dynamics in the simplest passive bipedal walking model," *J. Appl. Math. Modelling* **36**, 5262–5271 (2012).
7. A. Goswami, B. Thuilot and B. Espiau, "A study of the passive gait of a compass-like biped robot: Symmetry and chaos," *Int. J. Robot. Res.* **17**(12), 1282–1301 (1998).
8. M. Garcia, A. Chatterjee, A. Ruina and M. Coleman, "The simplest walking model: Stability, complexity, and scaling," *J. Biomech. Eng. Trans. ASME* **120**, 281–288 (1998).
9. M. Wisse, A. L. Schwab and F. C. T. Vander Helm, "Passive dynamic walking model with upper body," *Robotica* **22**(6), 681–688.

https://doi.org/10.1017/S0263574715000077 Published online by Cambridge University Press

10. R. P. Kumar, J. Yoon, Christiand and G. Kim, "The simplest passive dynamic walking model with toed feet: A parametric study," *Robotica* **27**, 701–713 (2009).
11. A. T. Safa, M. G. Saadat and M. Naraghi, "Passive dynamic of the simplest walking model: Replacing ramps with stairs," *J. Mech. Mach. Theory* **42**, 1314–1325 (2007).
12. Y. Hurmuzlu and G. D. Moskowitz, "The role of impact in the stability of bipedal locomotion," *Int. J. Dyn. Stab. Syst.* **1**(3), 217–234 (1986).
13. A. Goswami, B. Thuilot and B. Espiau, "Compass-like biped robot part I: Stability and bifurcation of passive gaits," *Institut National de Recherche en Informatique et en Automatique (INRIA), Technical Report*, (1996) p. 2996.
14. L. Ning, L. Junfeng and W. Tianshu, "The effects of parameter variation on the gaits of passive walking models: Simulations and experiments," *Robotica* **27**, 511–528 (2009).
15. A. Schwab and M. Wisse, "Basin of Attraction of the Simplest Walking Model," *Proceedings of Design Engineering Technical Conferences and Computers and Information in Engineering Conference*, Pittsburgh, Pennsylvania.
16. M. Wisse, *Essentials of Dynamic Walking, Analysis and Design of Tow-Legged Robots* (Delft University, Netherlands, 2004). ISBN 90-77595-82-1.
17. G. Berman and J. A. Ting, *Exploring Passive-Dynamic Walking* (Complex Systems Summer School, 2005).
18. J. Kim, C. H. Choi and M. W. Spong, "Passive Dynamic Walking with Symmetric Fixed Flat Feet," *International Conference on Control and Automation*, Guangzhou, China (May 30–1 Jun 2007).
19. Y. Jeon, Y. S. Park and Y. Park, "A study on stability of limit cycle walking model with feet: Parameter study," *Int. J. Adv. Robot. Syst.* **10**(49), (2013), doi: 10.5772/55162.
20. A. Chatterjee, M. Garcia, "Small slope implies low speed for McGeer's passive walking machines," *Dyn. Stab. Syst.* **15**, 139–157 (2000).
21. M. Kwan and M. Hubbard, "Optimal foot shape for a passive dynamic biped," *J. Theor. Biol.* **248**, 331–339 (2007).
22. J. Li, Y. Tian and H. Chen, "Foot Shape for Passive dynamic Kneed Biped Robot," *Proceedings of the IEEE International Conference on Robotics and Biomimetics*, Tianjin, China (December 14–18, 2010).
23. L. F. Shampine, I. GladWell and S. Thompson, *Solving ODEs with MATLAB*, (Cambridge, New York, 2003).

Appendix A. Models details

This appendix defines the equations of compass gait biped models as shown in Fig. 1.

A.1. Dynamics of the swing phase

For the point feet model:

$$M_n(\theta) = \begin{bmatrix} 1+\beta[(\overline{a}^2+\overline{b}^2+1)-2\overline{b}\cos\phi] & -\beta\overline{b}(\overline{b}-\cos\phi) \\ \overline{b}-\cos\phi & -\overline{b} \end{bmatrix}$$

$$C_n(\theta,\dot{\theta})\dot{\theta}+g(\theta) = \begin{bmatrix} \beta\overline{b}\dot{\phi}(2\dot{\theta}_{\mathrm{st}}-\dot{\phi})\sin\phi+\beta\overline{b}\sin(\theta_{\mathrm{st}}-\phi-\gamma)-(1+\beta(\overline{a}+1))\sin(\theta_{\mathrm{st}}-\gamma) \\ \dot{\theta}_{\mathrm{st}}^2\sin\phi+\sin(\theta_{\mathrm{st}}-\phi-\gamma) \end{bmatrix}.$$

For the curved feet model:

$$\begin{aligned} M_{n11} &= (1+\beta)[\overline{r}^2+(1-\overline{r})^2+2\overline{r}(1-\overline{r})\cos\theta_{\mathrm{st}}]+\beta[\overline{r}^2+(\overline{a}-\overline{r})^2+2\overline{r}(\overline{a}-\overline{r})\cos\theta_{\mathrm{st}}] \\ &\quad +\beta\overline{b}^2-2\beta\overline{b}[\overline{r}\cos(\theta_{\mathrm{st}}-\phi)+(1-\overline{r})\cos\phi] \\ M_{n12} &= \beta\overline{b}[-\overline{b}+\overline{r}\cos(\theta_{\mathrm{st}}-\phi)+(1-\overline{r})\cos\phi] \\ M_{n21} &= -\overline{b}+\overline{r}\cos(\theta_{\mathrm{st}}-\phi)+(1-\overline{r})\cos\phi \\ M_{n22} &= \overline{b} \end{aligned}$$

https://doi.org/10.1017/S0263574715000077 Published online by Cambridge University Press

$$
\begin{aligned}
C_{n11} + g_{n11} &= \beta\overline{b}\overline{r}(\dot{\theta}_{\mathrm{st}} - \dot{\phi})^2\sin(\theta_{\mathrm{st}} - \phi) + \beta\overline{b}(1-\overline{r})(2\dot{\theta}_{\mathrm{st}} - \dot{\phi})\dot{\phi}\sin\phi \\
&\quad + [(1+\beta)\overline{r}(1-\overline{r}) + \beta\overline{r}(\overline{a} - \overline{r})]\dot{\theta}_{\mathrm{st}}^2\sin\theta_{\mathrm{st}} + \overline{r}\sin\gamma - (1-\overline{r})\sin(\theta_{\mathrm{st}} - \gamma) \\
&\quad + \beta[2\overline{r}\sin\gamma - (\overline{a} + 1 - 2\overline{r})\sin(\theta_{\mathrm{st}} - \gamma) + \overline{b}\sin(\theta_{\mathrm{st}} - \phi - \gamma)] \\
C_{n21} + g_{n21} &= -[(1-\overline{r})\dot{\theta}_{\mathrm{st}}^2\sin\phi + \sin(\theta_{\mathrm{st}} - \phi - \gamma)].
\end{aligned}
$$

For the flat feet model:
First swing phase

$$
\begin{aligned}
\mathrm{M}_{n11} &= (1+2\beta)\overline{c}^2 + (1+\beta) + \beta(\overline{a}^2 + \overline{b}^2) - 2\beta\overline{b}(\overline{c}\sin\phi + \cos\phi) \\
\mathrm{M}_{n12} &= \beta\overline{b}(\overline{c}\sin\phi + \cos\varphi - \overline{b}) \\
\mathrm{M}_{n21} &= -(\overline{c}\sin\phi + \cos\varphi - \overline{b}) \\
\mathrm{M}_{n22} &= -\overline{b} \\
\mathrm{C}_{n11} &= \beta\overline{b}\dot{\phi}(\dot{\phi} - 2\dot{\theta}_{\mathrm{st}})(\overline{c}\cos\phi - \sin\phi) \\
\mathrm{C}_{n21} &= -(\overline{c}\cos\phi - \sin\phi)\dot{\theta}_{\mathrm{st}}^2 \\
g_{n11} &= \overline{c}\cos(\theta_{\mathrm{st}} - \gamma) - \sin(\theta_{\mathrm{st}} - \gamma) \\
&\quad + \beta[2\overline{c}\cos(\theta_{\mathrm{st}} - \gamma) - (\overline{a} + 1)\sin(\theta_{\mathrm{st}} - \gamma) + \overline{b}\sin(\theta_{\mathrm{st}} - \phi - \gamma)] \\
g_{n21} &= \sin(\theta_{\mathrm{st}} - \phi - \gamma).
\end{aligned}
$$

Second swing phase

$$
\begin{aligned}
\mathrm{M}_{n11} &= (1+2\beta)\overline{d}^2 + (1+\beta) + \beta(\overline{a}^2 + \overline{b}^2) + 2\beta\overline{b}(\overline{d}\sin\phi - \cos\phi) \\
\mathrm{M}_{n12} &= -\beta\overline{b}(\overline{d}\sin\phi - \cos\varphi + \overline{b}) \\
\mathrm{M}_{n21} &= \overline{d}\sin\phi - \cos\varphi + \overline{b} \\
\mathrm{M}_{n22} &= -\overline{b} \\
\mathrm{C}_{n11} &= -\beta\overline{b}\dot{\phi}(\dot{\phi} - 2\dot{\theta}_{\mathrm{st}})(\overline{d}\cos\phi + \sin\phi) \\
\mathrm{C}_{n21} &= (\overline{d}\cos\phi + \sin\phi)\dot{\theta}_{\mathrm{st}}^2 \\
g_{n11} &= -\{[\overline{d}\cos(\theta_{\mathrm{st}} - \gamma) + \sin(\theta_{\mathrm{st}} - \gamma)] \\
&\quad - \beta[2\overline{d}\cos(\theta_{\mathrm{st}} - \gamma) + (\overline{a} + 1)\sin(\theta_{\mathrm{st}} - \gamma) - \overline{b}\sin(\theta_{\mathrm{st}} - \phi - \gamma)]\} \\
g_{n21} &= \sin(\theta_{\mathrm{st}} - \phi - \gamma).
\end{aligned}
$$

A.2. Transition rules at collision
The matrices, Q_n^- and Q_n^+ for the point feet model are specified below:

$$
Q_n^- = \begin{bmatrix} (1+2\beta\overline{a})\cos\phi^- - 2\beta\overline{a}\overline{b} & \beta\overline{a}\overline{b} \\ -\overline{a} & 0 \end{bmatrix}
$$

$$
Q_n^+ = \begin{bmatrix} 1 + \beta(\overline{a}^2 + \overline{b}^2 + 1 - 2\overline{b}\cos\phi^+) & -\beta\overline{b}(\overline{b} - \cos\phi^+) \\ \overline{b} - \cos\phi^+ & -\overline{b} \end{bmatrix}.
$$

https://doi.org/10.1017/S0263574715000077 Published online by Cambridge University Press

The curved feet model

$$
\begin{aligned}
Q^{-}_{n_{11}} &= \overline{r}^2 + (1-\overline{r})^2\cos\phi^- + \overline{r}(1-\overline{r})(\cos\theta^-_{\mathrm{st}} + \cos(\phi^- - \theta^-_{\mathrm{st}}) \\
&\quad + \beta[2(\overline{r}^2 + \overline{b}(\overline{r}-\overline{a})) + \overline{r}(1+\overline{a}-2\overline{r})\cos\theta^-_{\mathrm{st}} + 2(1-\overline{r})(\overline{a}-\overline{r})\cos\phi^- \\
&\quad + \overline{r}(1+\overline{a}-\overline{b}-2\overline{r})\cos(\phi^- - \theta^-_{\mathrm{st}})] \\
Q^{-}_{n_{12}} &= \beta\overline{b}[\overline{a} - \overline{r}(1-\cos(\phi^- - \theta^-_{\mathrm{st}}))] \\
Q^{-}_{n_{21}} &= \overline{r}(1-\cos\theta^-_{\mathrm{st}}) - \overline{a} \\
Q^{-}_{n_{22}} &= 0
\end{aligned}
$$

$$
\begin{aligned}
Q^{+}_{n11} &= [1 - 2\overline{r}(1-\overline{r})(1-\cos\theta^+_{\mathrm{st}})] \\
&\quad + \beta[1 + \overline{b}^2 + \overline{a}^2 - 2\overline{r}(1+\overline{a}-2\overline{r})(1-\cos\theta^+_{\mathrm{st}}) - 2\overline{b}(\overline{r}cos(\phi^+ - \theta^+_{\mathrm{st}}) + (1-\overline{r})\cos\phi^+)] \\
Q^{+}_{n12} &= -\beta\overline{b}[\overline{b} - \overline{r}\cos(\phi^+ - \theta^+_{\mathrm{st}}) - (1-\overline{r})\cos\phi^+] \\
Q^{+}_{n21} &= \overline{b} - (1-\overline{r})\cos\phi^+ - \overline{r}\cos(\theta^+_{\mathrm{st}} - \phi^+) \\
Q^{+}_{n22} &= -\overline{b}.
\end{aligned}
$$

The flat feet model
First collision

$$
\begin{aligned}
Q^{-}_{n11} &= (1 - \overline{c}\overline{d}) + \beta[(1 + \overline{a}^2 - \overline{c}\overline{d}) + \overline{b}(-2\cos\phi + (\overline{d}-\overline{c})\sin\phi + \overline{b})] \\
Q^{-}_{n12} &= \beta\overline{b}(\cos\phi - \overline{d}\sin\phi - \overline{b}) \\
Q^{-}_{n21} &= \overline{b} - \cos\phi - \overline{c}\sin\phi \\
Q^{-}_{n22} &= -\overline{b}
\end{aligned}
$$

$$
\begin{aligned}
Q^{+}_{n11} &= (1 + \overline{d}^2) + \beta[(\overline{a}^2 + 1 + 2\overline{d}^2) + \overline{b}(2\overline{d}\sin\phi^+ - 2\cos\phi^+ + \overline{b})] \\
Q^{+}_{n12} &= \beta\overline{b}(\cos\phi - \overline{d}\sin\phi - \overline{b}) \\
Q^{+}_{n21} &= \cos\phi - \overline{d}\sin\phi - \overline{b} \\
Q^{+}_{n22} &= \overline{b}.
\end{aligned}
$$

Second collision:

$$
\begin{aligned}
Q^{-}_{n11} &= [(1 - \overline{c}\overline{d}) + 2\beta(\overline{a} - \overline{c}\overline{d})]\cos\phi^- - 2\beta\overline{a}\overline{b} - (\overline{d} + \overline{c})[1 + \beta(\overline{a}+1)]\sin\phi^- \\
Q^{-}_{n12} &= \beta\overline{a}\overline{b} \\
Q^{-}_{n21} &= -\overline{a} \\
Q^{-}_{n22} &= 0
\end{aligned}
$$

$$
\begin{aligned}
Q^{+}_{n11} &= (1 + \overline{d}^2) + \beta[(1 + \overline{a}^2 + \overline{b}^2 + 2\overline{d}^2) - 2\overline{b}(\overline{d}\sin\phi^+ + \cos\phi^+)] \\
Q^{+}_{n12} &= \beta\overline{b}(-\overline{b} + \overline{c}\sin\phi^+ + \cos\phi^+) \\
Q^{+}_{n21} &= \overline{b} - \overline{c}\sin\phi^+ - \cos\phi^+ \\
Q^{+}_{n22} &= -\overline{b}.
\end{aligned}
$$

https://doi.org/10.1017/S0263574715000077 Published online by Cambridge University Press

Appendix B

Matlab M-file for simulation of simplest walking model with point feet

```
Function Simplest_walking_point_Feet
%%%%%%%%%%%%%%%%%%%%%%%%%%%%%%%%%%%%%%%%%%%%%%%%
clc, clear all, close all, format long,
%%%%%%%%%% normal constant values%%%%%%%%%%%
gamma = 0.009;% slope of the walking surface
% x0 = [theta_stance; phi; thetadot_stance; phidot]
x0 = [.01; .02; -.01; 0];
%%%%%%%% Find proper initial conditions%%%%%%%%
tstart = 0; tfinal = 1e2;tout1 = tstart;
xout1 = x0.'; teout1 = []; xeout1 = []; ieout1 = [];
options1 = odeset('event', @collision1, 'RelTol', 1e-12, 'AbsTol', 1e-12);
for i = 1 : 50
% Solve until the first terminal event by ODE15s
sol_1_ode = ode45(@swing_stage,[tstart, tfinal],x0,options1);
t1 = sol_1_ode.x'; x1 = sol_1_ode.y'; te1 = sol_1_ode.xe'; xe1 = sol_1_ode.ye'; ie1 = sol_1_ode.ie';
nt = length(t1); tout1 = [tout1;t1(2:nt)]; xout1 = [xout1;x1(2:nt,:)];
teout1 = [teout1; te1]; xeout1 = [xeout1; xe1]; ieout1 = [ieout1; ie1];
% Normal Jump conditions
QP1 = [1 0; 1-cos(2*x1(end,1)) -1];
QN1 = [cos(2*x1(end,1)) 0; 0 0];
H1 = QP1 QN1;
x0(1,1) = -x1(end, 1);
x0(2,1) = -2*x1(end,1);
x0(3 : 4,1) = H1*[x1(end,3); x1(end,4)];
tstart = t1(nt);
end
figure(1), subplot(221), plot(tout1, xout1(:,1)), xlabel('time (sec), (l/g)^1^/^2'), ylabel('\theta_s_t (rad)')
subplot(222), plot(tout1, xout1(:,2)), xlabel('time (sec), (l/g)^1^/^2'), ylabel('\phi (rad)')
subplot(223), plot(tout1, xout1(:,3)), xlabel('time (sec), (l/g)^1^/^2'), ylabel('\theta^\cdot_s_t (rad/s)')
subplot(224), plot(tout1, xout1(:,4)), xlabel('time (sec), (l/g)^1^/^2'), ylabel('\phi^\cdot (rad/s)')
figure(2), subplot(121), plot(xout1(:,1), xout1(:,3)), xlabel('\theta (rad)'), ylabel('\theta^ \cdot (rad/s)'), axis tight,
subplot(122), plot(xout1(:,2), xout1(:,4)), xlabel('\phi (rad)'), ylabel('\phi^\cdot (rad/s)'), axis tight,
%%%%%%%%%%%%%%%%%%%%%%%%%%%%%%%%%%%%%%%%%%%%%%%%
solinit_bvp.x = sol_1_ode.x;solinit_bvp.y = sol_1_ode.y;solinit_bvp.parameters = pi;
sol_bvp = bvp4c(@bipedbvp, @bipedbc, solinit_bvp);
T1 = sol_bvp.parameters;t_bvp = T1*sol_bvp.x;t_bvp = t_bvp-t_bvp(1);T = t_bvp(end)
figure (3), subplot(121), plot (t_bvp, sol_bvp.y(1,:), 'r', t_bvp, sol_bvp.y(2,:),'b'), grid on, axis tight,xlabel('time (sec), (l/g)^1^/^2'),ylabel('\theta_s_t, \phi'),h = legend('\theta_s_t','\phi');
subplot (122), plot (t_bvp, sol_bvp.y(3,:), 'r', t_bvp, sol_bvp.y(4,:),'b'), grid on, axis tight,xlabel('time (sec), (l/g)^1^/^2'),ylabel('\theta^\cdot_s_t, \phi^\cdot'),h = legend('\theta^\cdot_s_t','\phi^\cdot');
%%%%%%%%%% Find period-one gait cycles%%%%%%%%%%
x02 = sol_bvp.y(:,1);
xout2 = []; tout2 = []; teout2 = []; xeout2 = []; ieout2 = [];
options2 = odeset('event', @collision2, 'RelTol', 1e-12, 'AbsTol', 1e-12);
for i = 1:5
sol_2_ode = ode15s(@swing_stage,[tstart, tfinal],x02,options2);
t2 = sol_2_ode.x'; x2 = sol_2_ode.y'; te2 = sol_2_ode.xe'; xe2 = sol_2_ode.ye'; ie2 = sol_2_ode.ie';
nt = length(t2);tout2 = [tout2;t2(2:nt)];xout2 = [xout2;x2(2:nt,:)];
teout2 = [teout2; te2]; xeout2 = [xeout2; xe2]; ieout2 = [ieout2; ie2];
% Normal Jump conditions
QP2 = [1 0; 1-cos(2*x2(end,1)) -1];QN2 = [cos(2*x2(end,1)) 0; 0 0];
H2 = QP2 QN2;
```

https://doi.org/10.1017/S0263574715000077 Published online by Cambridge University Press

```
x02(1,1) = -x2(end, 1);x02(2,1) = -2*x2(end,1);
x02(3 : 4,1) = H2*[x2(end,3); x2(end,4)];
tstart = t2(nt);
end
figure(4),subplot(121), plot (tout2, xout2(:,1),tout2, xout2(:,2),'–'),xlabel('time (sec)'), ylabel('Leg
angles (rad)'),grid on, axis tight,h = legend(' \theta_s_t','\phi ');
subplot (122), plot (xout2(:,1), xout2(:,3),xout2(:,2),xout2(:,4),'–'), xlabel('Leg angles (rad)'),
ylabel('Angular Velocities (rad/s)'),h = legend('Stance Leg','Swing Leg ');
%%%%%%%%%%%%%%%%%%%%%%%%%%%%%%%%%%%%%%%%%%%%%%%%%
functiondxdt = swing_stage(t,x)
M = [1 0; 1-cos(x(2)) -1];
N = [sin(gamma-x(1)); x(3)^2*sin(x(2))+sin(x(1)-x(2)-gamma)];
C = -Mn;
dxdt(1,1) = x(3);dxdt(2,1) = x(4);dxdt(3,1) = C(1,1);dxdt(4,1) = C(2,1);
end
%%%%%%%%%%%%%%%%%%%%%%%%%%%%%
function [value,isterminal,direction] = collision1(t,x)
value = cos(x(1))-cos(x(2)-x(1));isterminal = 1;direction = -1;
end
%%%%%%%%%%%%%%%%%%%%%%%%%%%%%
function [value,isterminal,direction] = collision2(t,x)
value = -x(2)+ 2*x(1);isterminal = 1;direction = -1;
end
%%%%%%%%%%%%%%%%%%%%%%%%%%%%%
functiondydx = bipedbvp(x,y, T)
M = [1 0; 1-cos(y(2)) -1];
N = [sin(gamma-y(1)); y(3)^2*sin(y(2))+sin(y(1)-y(2)-gamma)];
C = -Mn;
dydx = [T*y(3); T*y(4); T*C(1); T*C(2)];
end
%%%%%%%%%%%%%%%%%%%%%%%%%%%%%
function res = bipedbc(ya,yb,T)
QP = [1 0; 1-cos(ya(2)) -1];
QN = [cos(yb(2)) 0; 0 0];
H = QP QN;
res = [ya(1)+yb(1)
ya(2)+2*yb(1)
ya(3)-(H(1,1)*yb(3)+H(1,2)*yb(4))
ya(4)-(H(2,1)*yb(3)+H(2,2)*yb(4))
ya(2)+yb(2)];
end
end
```

https://doi.org/10.1017/S0263574715000077 Published online by Cambridge University Press